ELSEVIER

Journal of Structural Geology 26 (2004) 2073–2087

JOURNAL OF STRUCTURAL GEOLOGY

www.elsevier.com/locate/jsg

Rotation of uniaxial ellipsoidal particles during simple shear revisited: the influence of elongation ratio, initial distribution of a multiparticle system and amount of shear in the acquisition of a stable orientation

E. Cañón-Tapia*, M.J. Chávez-Álvarez

CICESE, Department of Geology, P.O. Box 434843, San Diego, CA 92143-4843, USA

Received 30 May 2003; received in revised form 17 February 2004; accepted 9 March 2004

Available online 20 May 2004

Abstract

The rotation of uniaxial ellipsoidal particles has provided the base for many studies of shape preferred orientations of mineral grains in a large variety of rock types. In this paper we present reports of a study of the evolution of a multiparticle system as a function of the elongation ratio of the particles and of the initial particle distribution. Our model reveals that both factors are important in controlling the acquisition of a stable orientation upon deformation. The more elongated particles (r = short axis/long axis ≤ 0.5) will define a stable fabric in almost any situation of geologic interest (γ = shear deformation < 10), but less elongated particles ($r > 0.5$) can also be considered to have achieved a stable orientation depending on the total amount of shear experienced by the rock. However, in systems with the less elongated particles ($r \geq 0.8$) it is possible to find mean orientations that are perpendicular to the direction of shear, although the occurrence of such behavior constitutes only a minor fraction of the studied examples. In any case, it is suggested that a systematic study of mineral fabrics in samples from the same rock can yield enough information to evaluate whether the mean shape preferred orientation of the minerals is parallel to flow direction.

Keywords: Mineral fabric; Shape preferred orientation; Shear strain

1. Introduction

The partitioning of deformation within a rock can be assessed through the analysis of shape preferred orientations (SPO) of mineral grains. Underlying these analyses is the mechanical behavior of rigid particles that are immersed in a moving viscous fluid. The basic equations describing such behavior were first established by Jeffery (1922), who also offered analytical solutions for the case of an axisymmetrical particle. These analytical solutions are more or less independent of the rheological characteristics of the fluid, as the only condition that must be satisfied is that of a linear velocity profile in the fluid (i.e. a Couette flow). Although in many geological situations the velocity profile to be considered is not linear, due to the small dimensions of the particles involved it is reasonable to use Jeffrey's solutions to predict the movement of a restricted part of the system. For example, the velocity profile of magma moving in a dike is parabolic near the walls of the intrusive (whether the magma rheology is considered Newtonian or Binghamian), but it can be approximated by a linear velocity profile in the vicinity of the small crystals floating in the magma. Consequently, one set of the equations derived by Jeffery only will be applicable to predict the motion of one section of the dike, like for instance close to one of its walls. A different set of equations with a different value of the velocity profile, however, can be used to investigate the motion of particles floating in a different part of the dike, like for instance closer to its center. The model derived by Jeffery (1922) is also applicable to deformation acquired in the solid state as long as the individual minerals defining the fabric of interest remain undeformed and the linear approximation of the velocity profile can be justified; conditions that are reasonably fulfilled in many cases of geological interest. Actually, departures from the ideal case depicted by Jeffery's equations are more likely to be due to the effects of mechanical interactions between neighboring

* Corresponding author. Tel.: +52-646-175-05-00, ext. 26049; fax: +52-646-175-05-59.

E-mail address: ecanon@cicese.mx (E. Cañón-Tapia).

0191-8141/$ - see front matter © 2004 Elsevier Ltd. All rights reserved.
doi:10.1016/j.jsg.2004.03.004

particles in the case of polycrystalline rocks than to rheological effects associated with a non-linear viscosity of the deformable phase. Consequently, the basic equations describing the mechanical behavior of rigid particles as established by Jeffery (1922) remains a useful tool to assess the partitioning of deformation within a rock through SPO analyses.

There are some characteristics of Jeffery's model that have received more attention than others in the geological literature. In particular, it has been emphasized very often that Jeffery's equations predict the rotation of an ellipsoidal particle with increasing strain. Upon rotation, the particle axis describes a closed trajectory in three-dimensional space whose amplitude depends on its initial orientation and on the particle aspect ratio. At first sight, such periodic movement is incompatible with the prominent mineral lineations or foliations observed in many rocks because these imply the achievement of a stable particle orientation. It was because of this characteristic of the model that Gay (1966, 1968) modified the conditions originally examined by Jeffery (1922) to derive a set of equations that predict a stable particle orientation as a function of increasing strain. The main change introduced by Gay (1966, 1968) consisted of considering a pure shear regime instead of the simple shear originally described by Jeffery (1922). Reed and Tryggvason (1974) extended Jeffery's and Gay's results (both valid only for one particle) to multiparticle systems. In complete analogy with the case of a single particle, they concluded that the degree of alignment in systems formed by axisymmetric particles increases monotonically for pure shear deformation whereas in simple shear the particles continue to oscillate indefinitely. The results obtained by Gay (1966, 1968) and Reed and Tryggvason (1974) showed that particle rotation is closely associated with the style of deformation, and somehow fostered the idea that a stable orientation could not be achieved if deformation had occurred as simple shear.

Contrary to this notion, it has been shown on several occasions that factors other than the style of deformation can also influence the periodic movement of an axisymmetric particle. For instance, Bretherton (1962) and Ildefonse et al. (1997) have shown that a stable particle orientation can be achieved in simple shear regimes provided that special conditions are satisfied, including (1) a fully 3D deformation regime, (2) a system formed by particles of different aspect ratio, or (3) mechanical interactions between particles. Notably, Manga (1998) proposed that a stable average orientation with increasing deformation can be achieved by a system of identical, very elongated particles experiencing simple shear in 2D, without any other special conditions imposed on it. Although the extremely elongated form of the particles considered by Manga (1998) is likely to be responsible for the acquisition of a stable preferred orientation of the system, his results are at odds with the oscillating behavior of a multiparticle system described by Reed and Tryggvason (1974). Such discrepancy in the behavior of multiparticle systems experiencing 2D simple shear remains unexplained until now.

Fernandez et al. (1983) further analyzed the periodic movement of a particle system, concluding that not only the orientation of individual particles rotates, but that the intensity of the fabric also changes periodically as deformation progresses. Based on such fluctuations of fabric intensity, they defined a critical amount of deformation that also behaves cyclically, although they considered that 'probably the only frequent {fabric} in nature' was related with the first cycle of fabric intensity or particle orientation. Consequently, if inferences drawn from SPO studies in geological situations were to be made reliably it would suffice to be certain that the first value of the critical deformation had not been exceeded. Unfortunately, so much emphasis is given to the rotational aspect of particle evolution that the implications of the existence of a critical deformation have been almost completely overlooked in subsequent works, and very little is currently known about the geological conditions under which a periodic movement of particles is actually significant.

In this paper we reexamine the role played by the aspect ratio of individual particles in the evolution of a multiparticle system that is experiencing simple 2D shearing. The results of our model allow us to reconcile the apparently opposite results of Manga (1998) and Reed and Tryggvason (1974). Additionally, in agreement with Fernandez et al. (1983), we were able to identify a threshold elongation ratio controlling the transition from an oscillating movement to a stable orientation. The significance of such a threshold value is explored within the context of different situations of geological interest, allowing us to define a significance-range depending on the total amount of shear that is likely to have been experienced by the rock under examination. Finally, our modeling approach allowed us to show that in systems formed of less elongated particles the initial distribution of the particle-axes (variable previously neglected) is extremely important in determining the evolution of the system. Consequently, we emphasize that all three factors (particle elongation, initial distribution and amount of shear considered) determine the type of fabric that can be achieved upon deformation.

2. Mechanical model of particle movement

Over 80 years ago, Jeffery (1922) established the equations of motion of rigid grains subject to forces exerted by a moving fluid along its surface. These equations can be used to estimate the angular velocity of the grain (ω) as a function (1) of the ellipsoid axes (A, B, C), (2) of the components of the strain rate tensor (d, f, g), and (3) of the

components of the vorticity tensor (ξ, β, ζ):

$$(B^2 + C^2)\omega_x = B^2(\xi + f) + C^2(\xi - f)$$
$$(C^2 + A^2)\omega_y = C^2(\beta + g) + A^2(\beta - g) \quad (1)$$
$$(A^2 + B_2)\omega_z = A^2(\zeta + d) + B^2(\zeta - d)$$

These equations must be solved numerically (e.g. Freeman, 1985; Hinch and Leal, 1979; Jezek, 1994) unless some simplifying assumption is introduced, in which case it is possible to find analytical solutions. For instance, Dragoni et al. (1997) solved these equations considering an axisymmetric particle (i.e. $A = C$ in Eq. (1)). They expressed the solutions in terms of Euler angles θ and ϕ (Fig. 1):

$$\tan\phi = r\tan\left[\frac{r\dot{\gamma}t}{r^2+1} + \arctan\left(\frac{1}{r}\tan\phi_0\right)\right]$$
$$\tan^2\theta = \frac{r^2\cos^2\phi_0 + \sin^2\phi_0}{r^2\cos^2\phi + \sin^2\phi}\tan^2\theta_0 \quad (2)$$

where $r = A/B$ is the elongation ratio of the grain, t is time, and θ_0, ϕ_0 denote the initial orientation of the particle. An advantage of using the solutions provided by Dragoni et al. (1997) is that by noting that the product $\dot{\gamma}t = \gamma$ is the total strain in Eq. (2) it is possible to produce all the output diagrams in terms of γ units (i.e. in terms of the amount of shear strain that has been exerted on the rock). Selection of γ to present the results not only avoids the problem of selecting an adequate shear rate to model a specific process, but also facilitates the interpretation of the results in a geological context by focusing on a parameter that is easier to quantify, as is deformation.

Based on Eq. (2), we wrote a MATLAB code to examine the evolution of a multiparticle system as a function of increasing deformation. Similar to codes used in other fabric studies (e.g. Jezek, 1994; Dragoni et al., 1997; Iezzi and Ventura, 2002), our code allows us to assign the particle elongation ratio, but unlike that used in previous works, our code is more flexible in the evaluation of the influence of the initial distribution of particle axes in the evolution of a fabric. This flexibility is accomplished by generating a nearly uniform, aleatory initial distribution of 200 axes each time the program starts to run. The initial distribution can be saved, and fed into the program as a starting point at any other time if desired, therefore assuring reproducibility of the results. Alternatively, any given distribution of interest can be used as an initial distribution in our code.

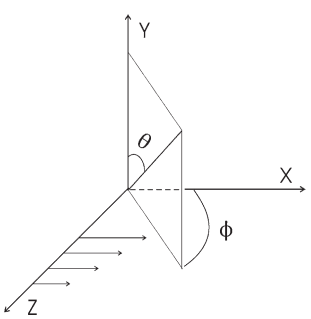

Fig. 1. Diagram showing the orientation of the Euler angles (θ and ϕ) and of the simple shear (arrows) considered here.

A quantitative measure of the average orientation of axes and of the shape and strength of the fabric is obtained by calculating the orientation matrix and associated parameters (Woodcock, 1977). This calculation is made for the initial distribution and for each of the subsequent distributions obtained by solving Eq. (2) for each particle upon an increment of the total strain (i.e. $\gamma = 0, 1, 2, 3\ldots$). The number of steps to be modeled is fixed at the beginning of each run, but can be easily adjusted in our code to suit the needs of a particular set of parameters.

Using this code, a total of 600 initial (random) distributions were generated for prolate grains and another 600 for oblate grains. These distributions included elongation (flattening) ratios in the range $r =$ minimum axis of the ellipsoid/maximum axis of the ellipsoid $= 0.05$–0.95. The results were found to be qualitatively equivalent for either prolate or oblate particles, as can be seen in the tables describing the time evolution of the axes of principal susceptibility of these systems reported elsewhere (Cañón-Tapia and Chávez-Álvarez, 2004). For this reason we only concentrate here on describing the results obtained from the prolate grains. In the following sections we first describe and discuss the effects observed in the fabric by changing the particle elongation-ratio independently of the initial orientation distribution of the system, and later focus on the effects of a changing initial orientation distribution. The significance of both of these results in a geologic context is examined later.

3. Effect of particle shape on the evolution of a multiparticle system

Three examples of the evolution of a system having the same initial distribution are shown in Figs. 2–4. Each of the diagrams in these figures is an equal area projection (lower hemisphere) showing the orientation of the 200 particle-axis that forms the system at a given deformation stage. The difference between the figures is the elongation ratio of the particles that form each system. The system shown in Fig. 2 is formed by particles that are nearly spherical ($r = 0.9$), whereas those forming the systems of Figs. 3 and 4 are increasingly elongated ($r = 0.5$ and 0.1, respectively). The snapshots of the system in each figure are shown at equal γ intervals to facilitate comparison between systems composed of particles of different shapes. It is observed that when $r = 0.9$ (Fig. 2), the initial distribution of axes change very little with increasing γ, although some degree of clustering is defined at each interval. The formation of axial clusters is better defined at specific γ values when the particles have $r = 0.5$ (e.g. $\gamma = 5$ and $\gamma = 13$ in Fig. 3), and

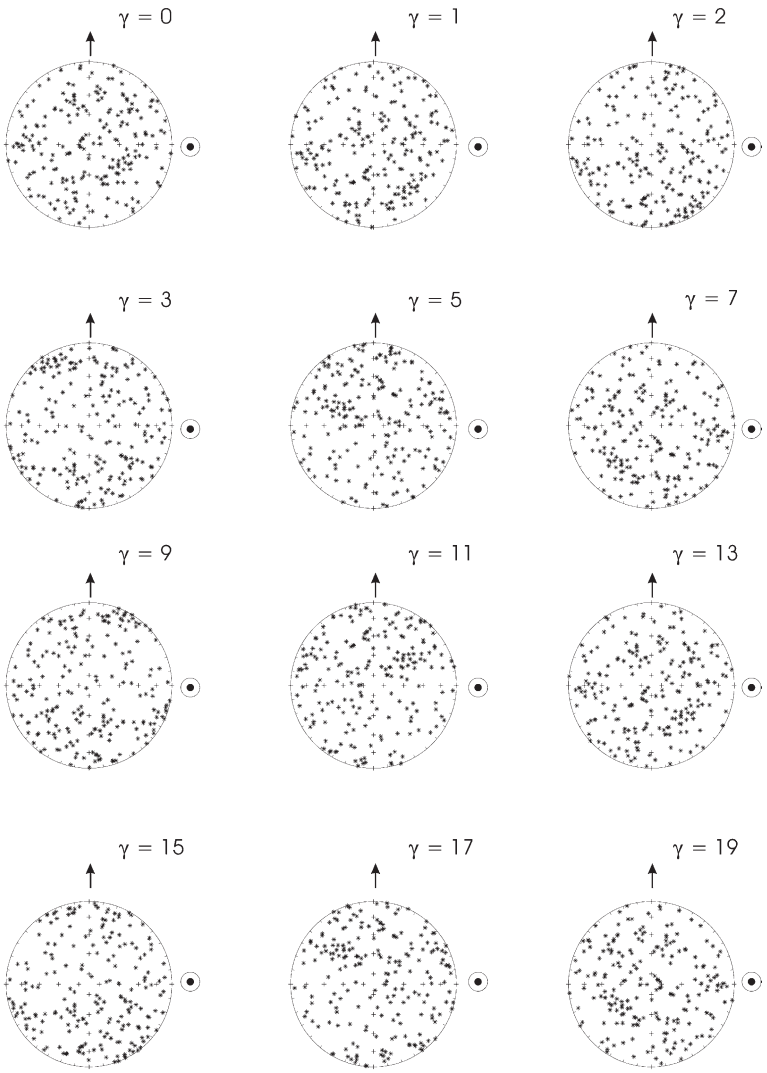

Fig. 2. Evolution of the distribution of mineral axes as a function of increasing shear. All diagrams in this figure are equal area projections (lower hemisphere) showing the orientation of the 200 axis at a given value of shear (γ). The orientation of the velocity (arrows) and its gradient ($\odot$), as defined in Fig. 1, are also indicated in each diagram. The particles of this system have an elongation ratio $r = 0.9$.

becomes a distinctive feature of the system when $r = 0.1$ (Fig. 4). Actually, the formation of clusters in this latter case is almost immediate, and the distribution of axes changes very slowly after the cluster is formed. For oblate particles, the evolution of the system would be similar to those shown in Figs. 2–4, except that the cluster of axes in the more unequant particles will be along the gradient of velocities rather than along the direction of shear.

The plot of Fig. 5 allows us to make a quantitative description of the axial distributions shown in Figs. 2–4 by plotting the ratios of the eigenvalues of the orientation matrix (Woodcock, 1977). In this figure it is observed that for the case $r = 0.9$ the distributions of axes at every time step is nearly isotropic, whereas most of the distributions formed by the system of particles when $r = 0.1$ are distinctively anisotropic. This figure also shows that most of the distributions of axes are close to the girdle–cluster transition, with a slightly better development of a girdle in the most anisotropic cases. In Fig. 6 we show the location of the S1 eigenvector of the orientation matrix, which roughly represents the mean direction of the distribution for prolate grains. In the case of oblate grains this direction would represent the normal to a grain-generated foliation. As seen in Fig. 6, the position of the mean moves from north to south along two trajectories well defined when $r = 0.9$, whereas in the case when $r = 0.1$ the mean remains almost stationary along the N–S direction. The case when $r = 0.5$ is intermediate between these two cases. It must be noted in Figs. 5 and 6 that although the trajectory defined by a system is well defined in each diagram, the evolution of the system is not linear in the sense that fabric intensity (and orientation) defines such trajectories upon several cycles and not in a progressive form.

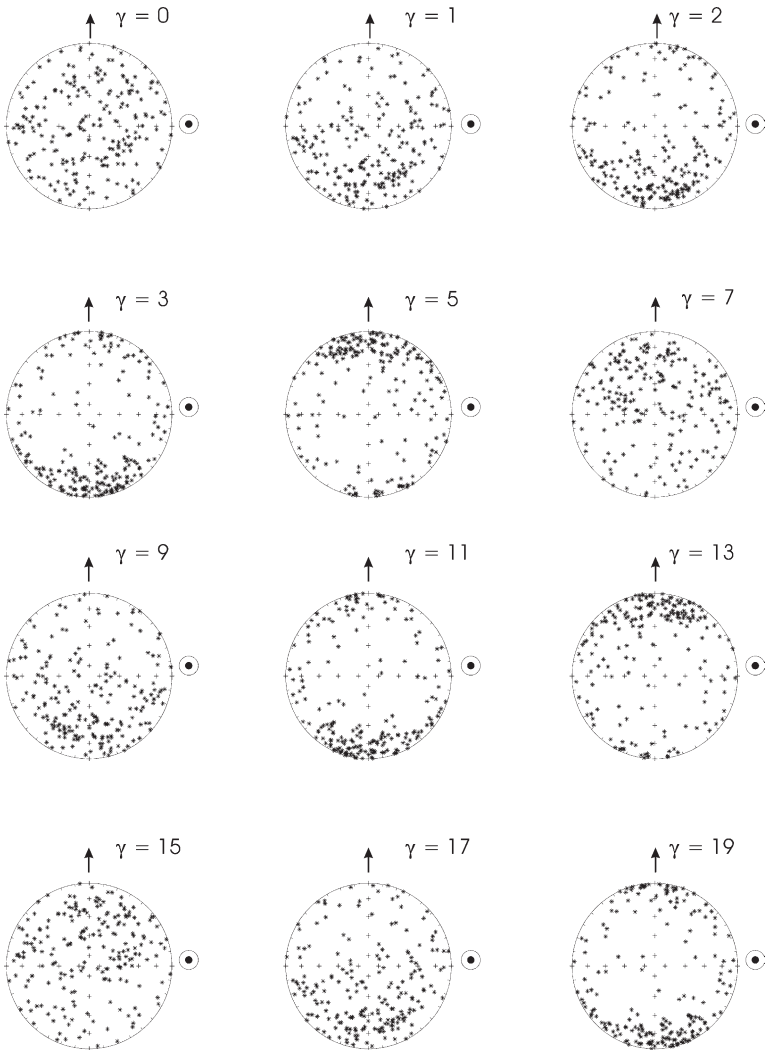

Fig. 3. Evolution of the distribution of mineral axes as a function of increasing shear. The distribution at $\gamma = 0$ and all symbols are the same as in Fig. 2. The particles of this system have an elongation ratio $r = 0.5$.

3.1. Frequency of rotation of a multiparticle system

According to the basic equations of movement (Jeffery, 1922), the axis of a single particle should describe a closed trajectory, the sense of rotation being determined by the orientation of both the velocity of the fluid and the gradient of velocities. In the cases depicted by Figs. 2–4, the velocity points to the north, and the gradient of velocities is vertical away from the plane of the page. These conditions produce the rotation of an isolated particle in a N–S sense in the lower hemisphere diagrams used in this paper. Consequently, the expected rotation of the whole system should also be from north to south. Although such behavior is clearly displayed by the intermediate case ($r = 0.5$; Fig. 3), the rotation of the system is difficult to observe in the case of more equant and of more elongated particles (Figs. 2 and 4, respectively). To interpret these observations, it is illustrative to take into consideration the characteristics of the movement of one isolated particle. As clearly shown by Dragoni et al. (1997), the velocity of rotation of a single particle is smaller when its axis is closer to the plane normal to the gradient of velocities (the horizontal plane in our diagrams) and faster when it is perpendicular to this plane. In any case, the ratio of the velocities parallel and perpendicular to the horizontal can reach a factor of about 20 when the particles are elongated, so that in multiparticle systems it gives opportunity for the particles that are perpendicular to the horizontal to ‘catch up’ with the particles that arrived there first. Such behavior results in a relatively stable orientation of axes within the horizontal plane. In contrast, when the particles are more equant the ratio of velocities of the same particle during its movement is one order of magnitude lower (very close to unity for the more spherical particles), and therefore many particles leave the horizontal plane before others have the time to accommodate in this position. For this reason, approximately the same number of particles remain within the horizontal and far from it at any given time, and consequently no net rotation of the collection of particles is observed. Therefore, in the cases of either very elongated

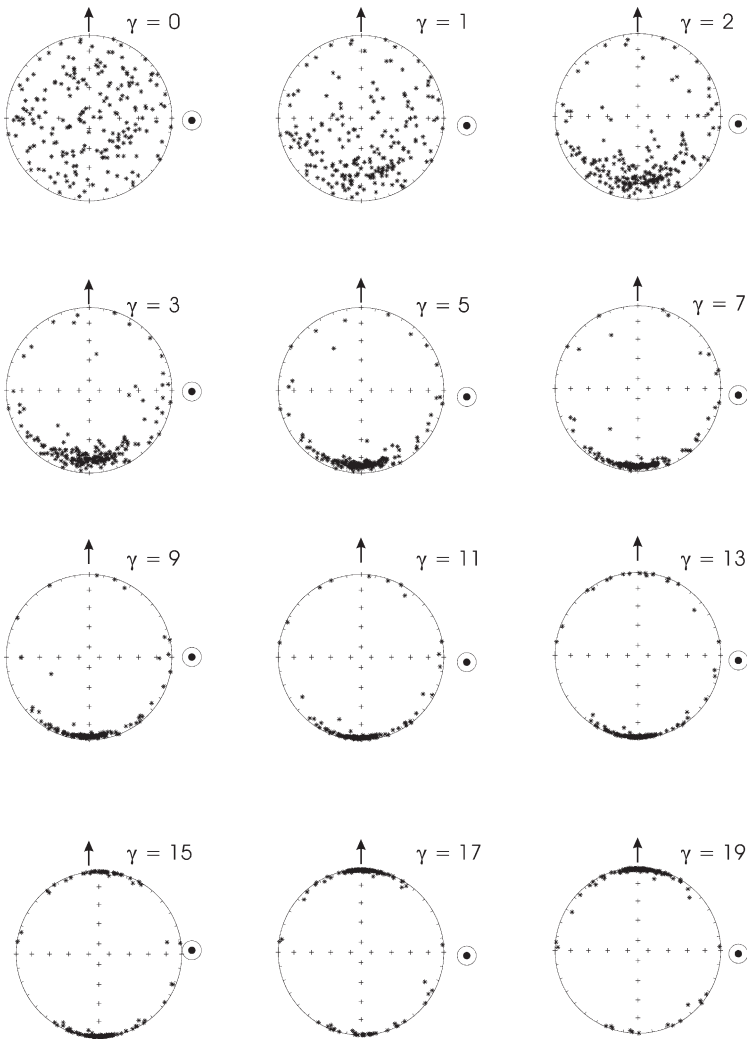

Fig. 4. Evolution of the distribution of mineral axes as a function of increasing shear. The distribution at $\gamma = 0$ and all symbols are the same as in Fig. 2. The particles of this system have an elongation ratio $r = 0.1$.

or almost equant particles the rotation predicted by the movement of one isolated particle is not easy to observe in the evolution of the system. For oblate particles this relationship is inverted, as very flattened particles will spend most of the time with their axis normal to the horizontal plane (for the conditions defined here).

By focusing on the evolution of systems in which shear orientation and rate do not change with time it is possible to find a characteristic period of rotation of particle system as a function of elongation ratio of the individual particles. This can be done in three alternative forms, the most direct of which involves a simple calculation of the period of one single particle (Fernandez et al., 1983; Jezek et al., 1994; Dragoni et al., 1997). Alternatively, the changing orientation of the axial mean direction or changes in the intensity of the axial fabric (represented by the larger eigenvalue of the orientation matrix and by the logarithm of the ratio of the larger to the smaller eigenvalues, respectively), can be used to define the period of rotation of the whole system. The first method is based on the fact that every particle in the system rotates with a characteristic period that is a function only of the particle elongation ratio. Consequently, two systems each formed by particles of the same ratio will have identical rotation periods. In contrast, if the period of rotation of the system is calculated by using any of the two alternative methods mentioned, two different systems will yield different signals as shown next.

Inspection of the trajectories defined by the axial means shown in Fig. 6, reveals that although the mean defines a closed trajectory, its position is not equally spaced along the trajectory. By projecting the axial mean direction at each γ into the plane formed by the flow velocity and its gradient, it is easy to find the shear intervals that result in a large difference in the orientation of the mean (Fig. 7). Commonly, the change in orientation of the axial mean in these diagrams will be associated with the 'jump' from 180° to 0° associated with the completion of one of the loops in the trajectory of the mean. Sometimes, however, a jump $>120°$ not associated with a flipping from north to south can be detected (e.g. triangles in Fig. 7B). If we define the

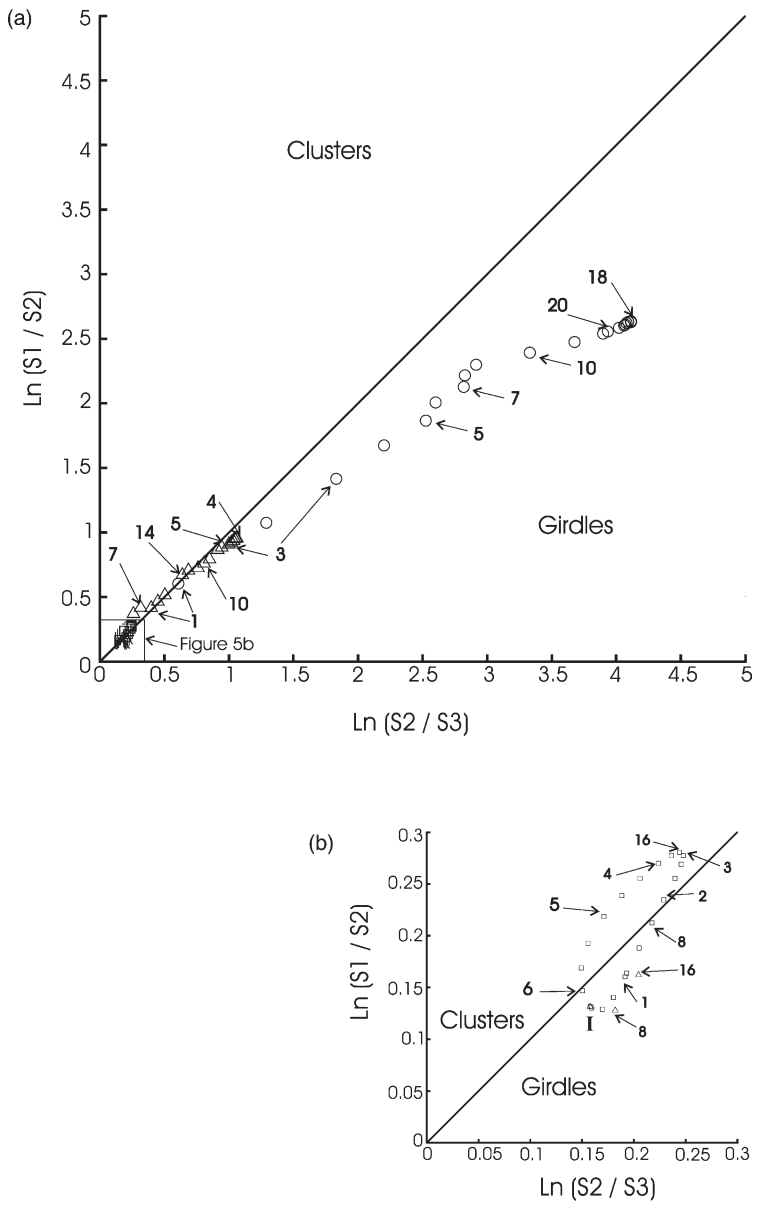

Fig. 5. Fabric intensity of the multiparticle systems shown in Figs. 2–4. S1–S3 are the eigenvalues of the orientation matrix obtained from the distribution of axis (Woodcock, 1977). Squares, triangles and circles represent the system when particles have $r = 0.9$, 0.5 and 0.1, respectively. Selected values of γ are indicated numerically in the figure; I indicates the position of the fabric of the initial distribution that is the same for all the three cases shown. A detail of the less intense fabrics is shown in (b).

characteristic period of rotation of the system as the average deformation required to produce a change in the orientation of the mean by more than 120°, there will be some systems with a period of rotation that depart from the period predicted for rotation of a single particle. Results of the calculation of the period of rotation based in the position of the axial mean for each of our 600 initial distributions, and for each elongation ratio, are shown in Fig. 8. In this figure both the mean and the median of the period of rotation at each value of r are plotted. The difference between these two variables results from a non-normal distribution of the period of rotation at a given r. For this reason, the interval shown at each r is not symmetric around the mean. The upper limit of the bars indicates the maximum period of rotation found in each of the 600 distributions examined at each r, whereas the lower limit is located one standard deviation below the mean. Nonetheless, due to the skewed form of the distribution of rotation periods, signaled by the coincidence of the median with the upper limit of the bars at all values of r, the whole interval marked by the bar contains more than 68% of the observations. Consequently, despite its asymmetry, the interval shown by the bars can be interpreted in the same form as a symmetric confidence interval of one standard deviation around the mean in a normal distribution.

Also included in Fig. 8 is the rotation period calculated

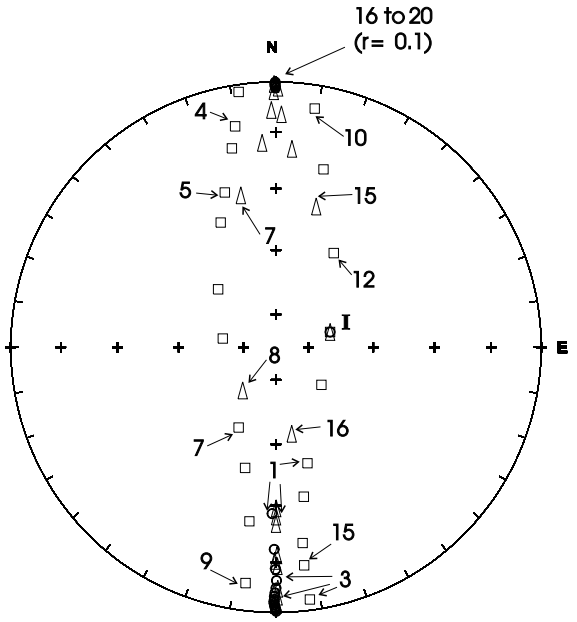

Fig. 6. Orientation of the mean direction of the multiparticle systems shown in Figs. 2–4. Selected values of γ are indicated numerically in the figure, and symbols are as in Fig. 5.

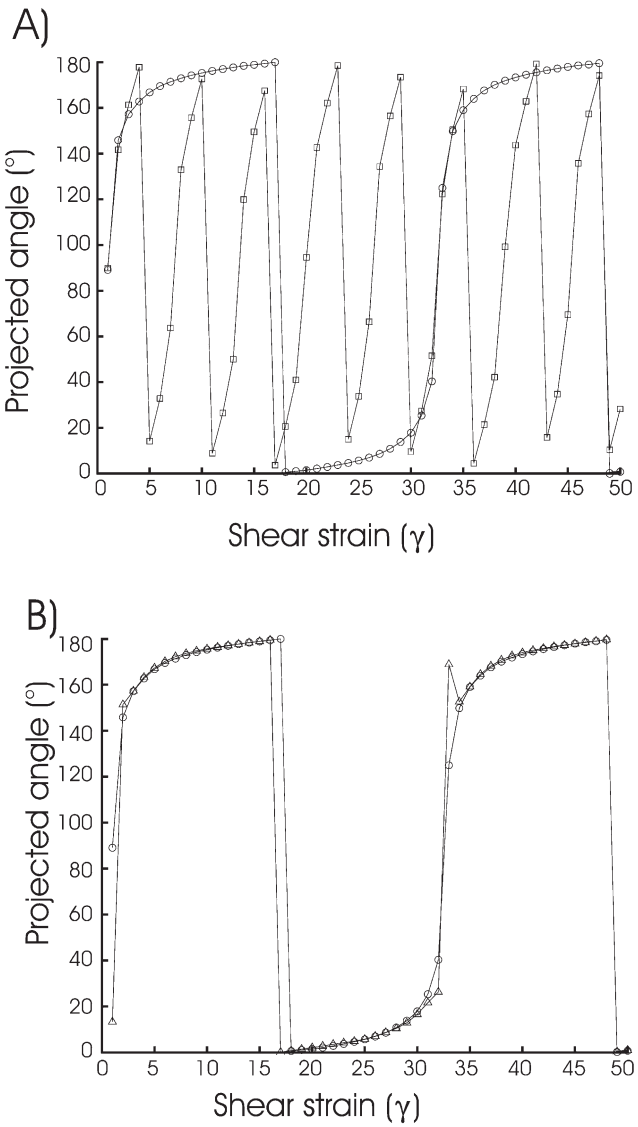

Fig. 7. Projection on the vertical N–S plane of the mean direction of multiparticle systems as a function of increasing strain. The two systems shown in (A) have identical initial distribution but different particle aspect ratio (circles: $r = 0.1$; squares: $r = 0.9$), whereas those shown in (B) have the same $r = 0.1$ but different initial distribution.

by considering an isolated particle. It can be observed in the figure that this period corresponds to the maximum period of rotation found by considering the change in the direction of the axial mean. In any case, it is found that the rotation period increases from its lowest value achieved for large values of r ($r > 0.60$) to a maximum value at $r = 0.05$, allowing us to define three distinctive zones in terms of the amount of shear strain that has occurred in the rock. The first of these zones includes situations in which shear strain remains below four. Even by taking into consideration the total intervals marked by the error bars in the figure, in this zone none of the systems will behave cyclically, regardless of the elongation ratio of the particles. If strain values between four and seven are considered, all systems formed by particles with an $r > 0.6$ would have completed at least half of one closed loop and therefore have a cyclic behavior, but particles with $r < 0.3$, and at least some systems formed by particles with $0.3 < r < 0.6$ will remain acyclic. For situations in which shear strain remains below 10, systems formed by very elongated particles ($r < 0.2$) can be safely considered as acyclic.

By focusing now on the fluctuations of the intensity of the axial fabric as a function of shear, it is found that although it is possible to find a dominant period (that in all cases coincides with the period of rotation characteristic of an isolated particle), any two systems might have a different fabric intensity at a given shear (Fig. 9). In particular, for the case of systems formed by more elongated particles, the differences can be expressed as higher frequency fluctuations in the intensity of the fabric that can be observed when the intensity is more anisotropic (Fig. 9A). Although these rapid fluctuations in the fabric intensity are not observed in the case of systems formed by more equant particles, the differences between two systems are still preserved, and in extreme cases the more anisotropic fabric of one system can be achieved at the same value of γ than the more isotropic fabric of another system (Fig. 9B). These results contrast with the implications of the 2D analysis made by Fernandez (1987), in which the maximum fabric intensity is exclusively found at the critical shear. The difference in results is due in part to the inclusion of the 3D movement of each particle in the calculations, but also reflects the effects of the initial distribution in the system evolution, variable that we now turn to examine with more detail.

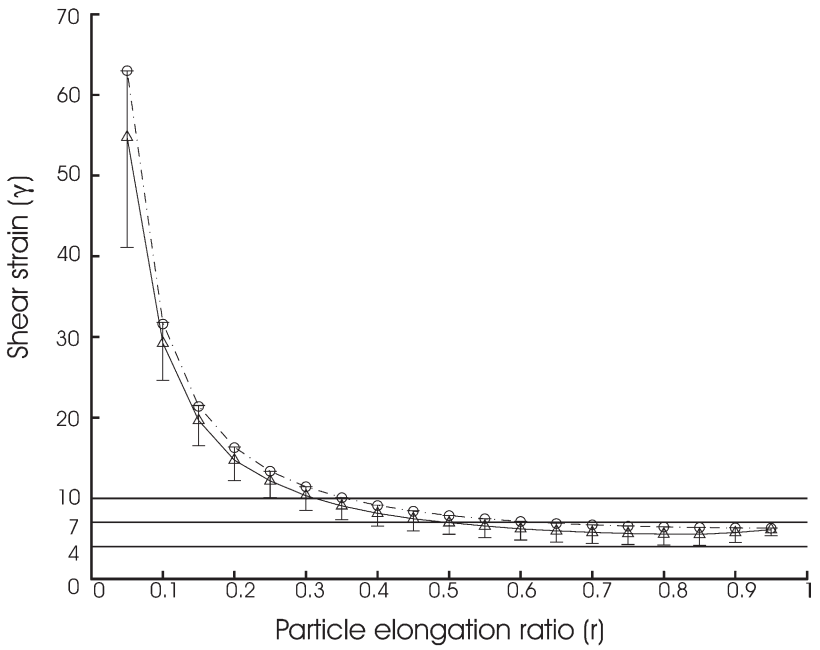

Fig. 8. Amount of shear strain required to complete one period of rotation by the multiparticle system as a function of particle elongation ratio. Triangles show the mean value and circles show the maximum period found. The dashed–dotted line represents the period of one single particle. See text for more details concerning the error bars.

4. Effect of the initial distribution on the system evolution

Examples of the influence that a different initial distribution has on the system evolution are shown in Figs. 10–12. Fig. 10A illustrates the evolution of two systems with identical elongation ratios ($r = 0.9$) but different initial distributions. Initially, one of the fabrics (squares) is within the field of girdles but as deformation progresses it moves towards the field of clusters, whereas the other fabric (triangles) is initially within the field of clusters and moves towards the field of girdles. Actually, there is some stage during their evolution in which both systems plot very close to each other. As the elongation ratio of the particles in this case is close to one, the rotation effects discussed in the previous section result in an oscillating behavior within the two most extreme fabric types displayed in the diagram. This means that even if deformation would increase beyond the 20γ units shown in Fig. 10A, the fabric would remain within the two extremes of the paths shown. Also, it is noted that not only the shape of the fabric can be contrastingly different, but also their attitudes. This is shown in Fig. 10B where it is observed that one of the distributions is characterized by a mean cluster direction along two paths nearly parallel to the N–S vertical plane whereas the other distribution yields mean directions normal to this plane.

The effect of the initial distribution on the evolution of the fabric just described remains valid, though less clear, for more elongated particles as shown in Figs. 11 and 12. To facilitate the discussion, the squares and triangles in Figs. 10–12 represent systems that have the same initial distributions in all three figures. The two systems shown in Fig. 11 have elongation ratios $r = 0.5$ whereas those shown in Fig. 12 have elongation ratios $r = 0.1$. In Fig. 11A, it is observed that the strength of the fabric increases for most of the deformation stages, and that the character of each remains distinctive most of the time. The orientation of the mean direction (Fig. 11B) remains almost constant most of the time, but it is still possible to find some stages of deformation in which the mean is normal to the flow direction for one of the initial distributions. In contrast, when the particles are very elongated (Fig. 12) the differences in the shapes and strengths of the fabrics are less clear in most stages of deformation, but still it is possible to find two fabrics with different characteristics at a given strain (Fig. 12A).

It is important to note that in addition to the effect introduced by the difference in the velocity of rotation of individual particles as a function of particle shape, the initial orientation of individual particles introduces some variability in the degree of clustering that can be achieved at any stage of deformation. For example, in Fig. 4 it is possible to observe a reasonably stable population of grains that remain perpendicular to flow. These individual grains are actually rotating, but the trajectory described by their axis is such that the particle axis does not move away in a noticeable form from the east direction. In the extreme case of an elongated particle with its axis originally oriented in the E–W direction, the axis will remain in that orientation for all values of deformation defining what can be called a ‘rolling’ effect. Within the context of the idealized model

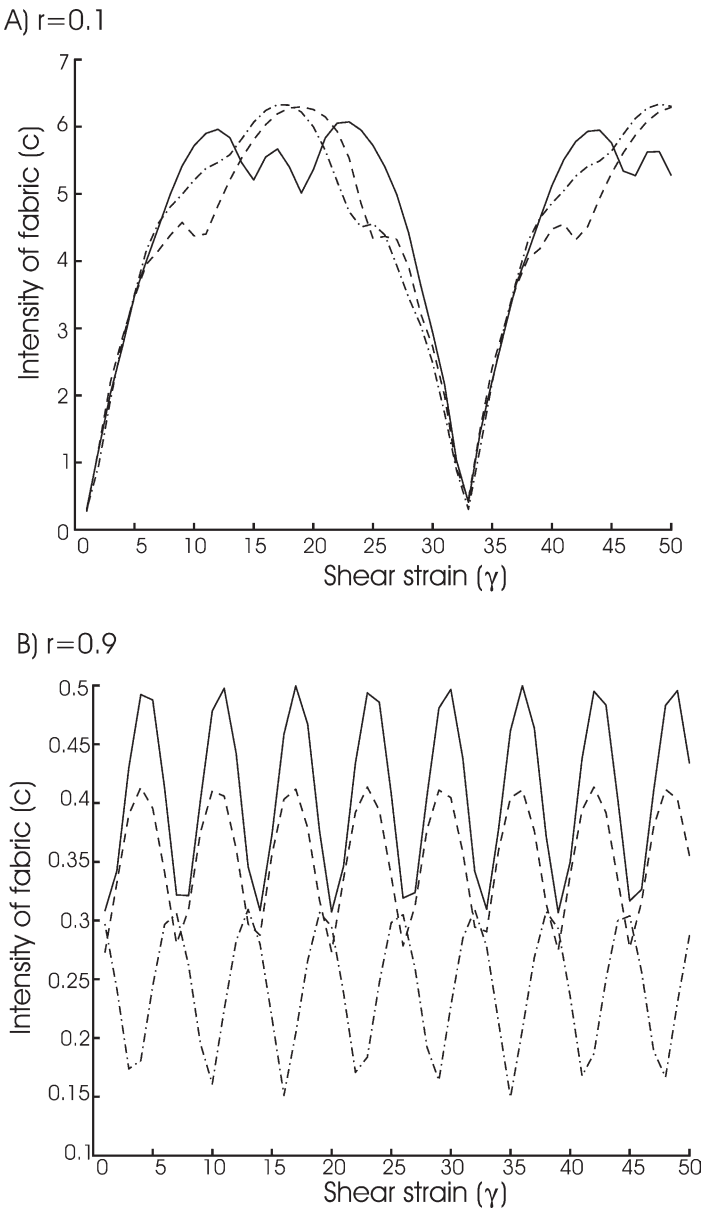

Fig. 9. Variation of the fabric intensity as a function of shear strain. The three systems shown in (A) have $r = 0.1$ but different initial distribution, whereas those in (B) have $r = 0.9$.

developed by Jeffery (1922), the only possibility to change the orientation of these particles would be a change in the orientation of shear with time. The effect of such change in the direction of shear in the whole system would depend on the exact timing at which it takes place, as the 'initial' orientation of the system may not be as aleatory as supposed here. Another aspect that must be considered is the formation of small clusters on the initial distribution. These clusters are the result of the aleatory procedure used to create the initial distribution, and include some probable effects of bias in the generation of random numbers from the MATLAB command. The presence of such clusters is not important in the present context, however, as suggested by the weak intensities defined by the orientation tensor eigenvalues. Besides, in natural situations it is probable that very localized processes during crystal formation could induce the formation of crystals with similar orientation in small volumes. For this reason, a completely uniform distribution may not be defined even if a much larger number of crystals than that used here was considered.

Even when these restrictions imposed by the numerical procedure used to generate our 600 initial distributions are taken into consideration, some general features of our systems can be identified. For example, all of our model results show that the expected cyclic behavior of the system indeed is a function of the aspect ratio of the particles. Most importantly, they highlight the role played by the amount of

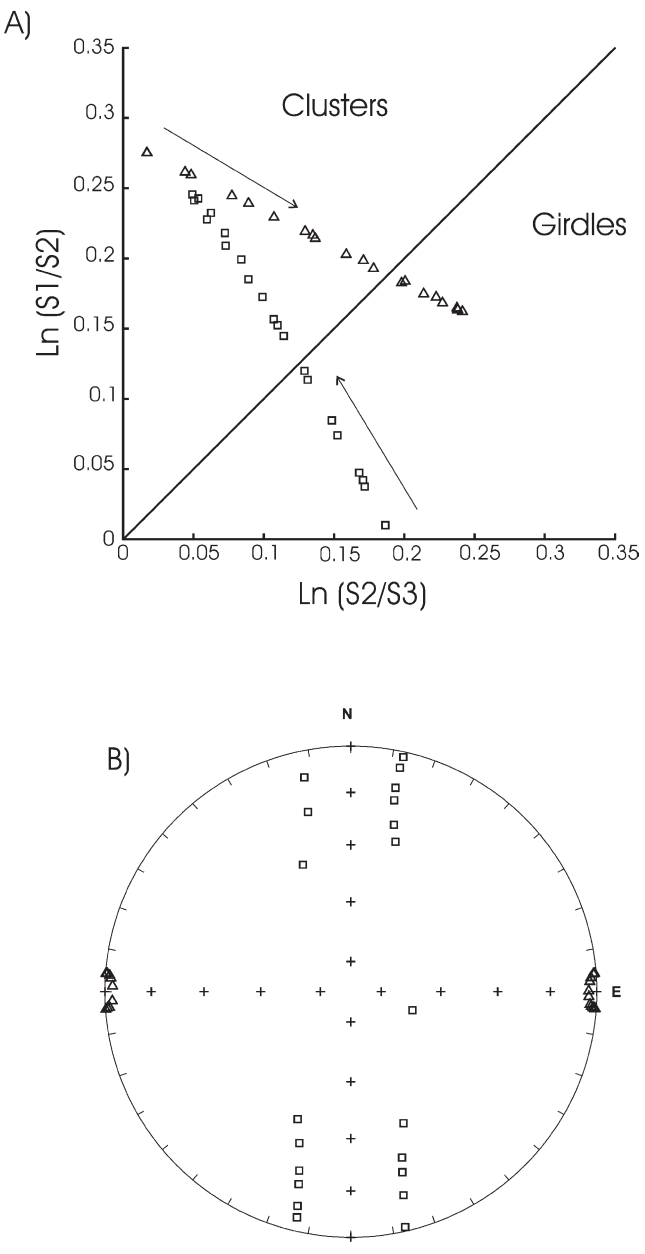

Fig. 10. Examples of the fabric evolution ((A) intensity and (B) orientation of the mean) of two systems with different initial distributions and $r = 0.9$. The arrows in (A) indicate the direction of the initial evolution of the fabric.

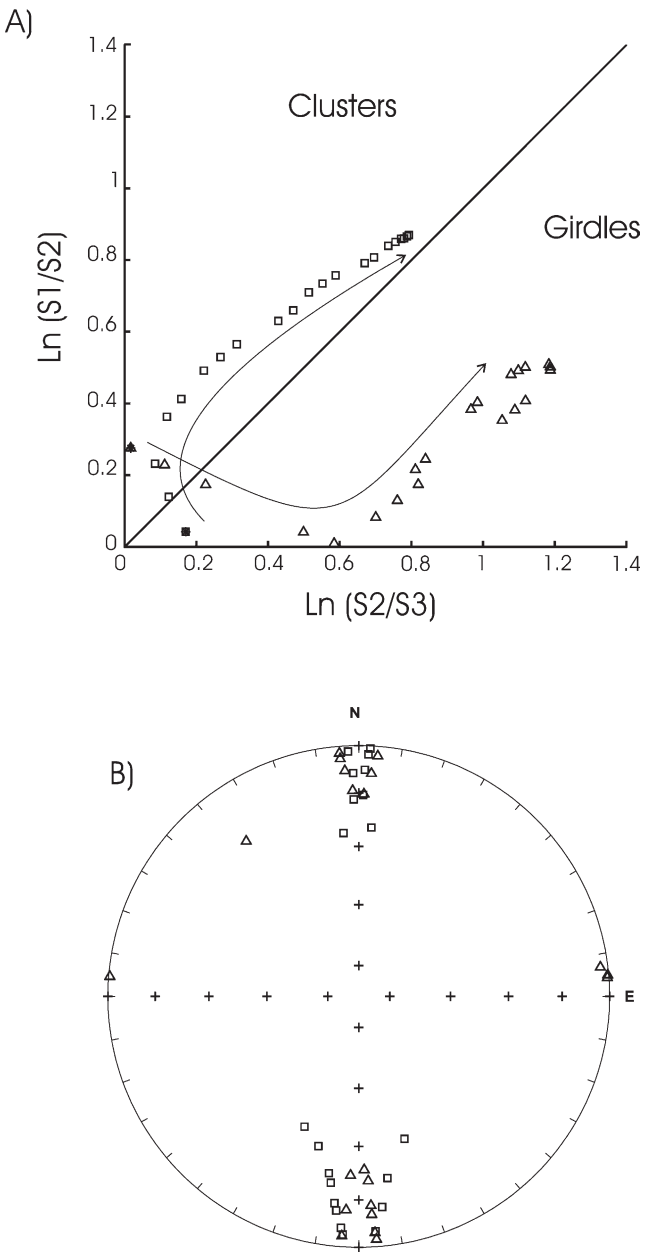

Fig. 11. Examples of the fabric evolution ((A) intensity and (B) orientation of the mean) of two systems with different initial distributions and $r = 0.5$. The initial distribution of each of these systems is the same as the distribution of the system with the same symbol shown in Fig. 10. The arrows in (A) indicate the direction of the initial evolution of the fabric.

shear considered in each situation and by the distribution of the system at the reference value of zero shear. All of these factors are likely to be important in the interpretation of fabrics observed in real rocks as discussed next.

5. Discussion

Previous studies concerning the acquisition of a SPO of a group of particles have focused their attention on describing the effect of different deformation styles (Reed and Tryggvason, 1974; Freeman, 1985; Iezzi and Ventura, 2002). Much emphasis has been given in these studies to show that pure shear promotes the acquisition of a stable fabric whereas a periodic rotation is to be expected for simple shear. In contrast, our results show that although rotation of the system is a characteristic of deformation under simple shear regimes, a key element in deciding whether the fabric can be considered stable or not is the amount of deformation that is experienced by the particular rock. Another important aspect of our model concerns the ability of SPO to record the orientation of shear. In this particular context, our results show that for the cases of

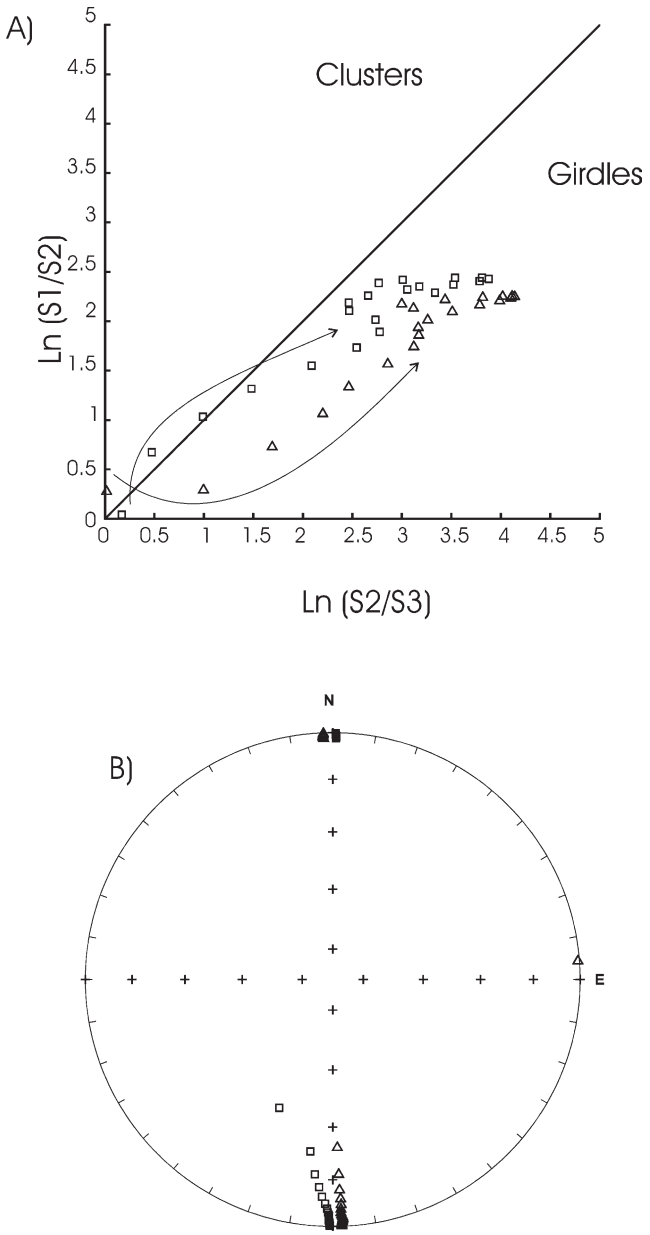

Fig. 12. Examples of the fabric evolution ((A) intensity and (B) orientation of the mean) of two systems with different initial distributions and $r = 0.1$. The initial distribution of each of these systems is the same as the distribution of the system with the same symbol shown in Figs. 10 and 11. The arrows in (A) indicate the direction of the initial evolution of the fabric.

more equant particles the problem is not so much whether the particles completed one cycle (especially true if only small amounts of γ are considered, as already pointed out by Fernandez et al. (1983)), but rather what is the initial distribution of those particles at the time considered to be of zero deformation. The implications of these two model results are now examined with regard to more specific geologic situations.

5.1. Amount of deformation and fabric evolution

The interest in the SPO of markers in rocks traditionally has formed part of the study of metamorphic and plutonic rock textures. Increasing interest in the processes controlling the emplacement of volcanic and shallow intrusive rocks, however, has resulted in attempts to apply these methods in a wide range of deformation scenarios, including conditions that differ in the rate of shear by several orders of magnitude (Smith, 2002). More important, perhaps, is the total amount of deformation that must be considered in each situation. For example, the distance traveled by an individual crystal floating in magma that is ascending through a dyke is on the order of kilometers, and consequently even a small difference in velocity between adjacent fluid elements (and hence a small shear rate) can result in large amounts of total shear strain. On the contrary, in granitic or metamorphic rocks that are likely to have traveled relatively small distances during deformation, small values of shear rate will result in comparably smaller amounts of total shear strain despite the larger times involved.

Commonly, the displacement of individual markers can be assessed depending on the situation of interest and consequently a practical upper limit for γ can be estimated. Although shear strains of up to 40 can be measured in narrow zones with special evolutionary histories like some mylonite belts, total strains <5 are considered to be large enough to cover most shear strain in granitic rocks during intrusion and other deformational settings, and therefore an upper limit of $\gamma \sim 10$ is commonly considered suitable for most metamorphic and plutonic rocks (Pfiffner and Ramsay, 1982; Fernandez and Fernández-Catuxo, 1997). If we consider the movement of magma through a dyke, or of a lava flow or dome on the surface, however, we might have to consider a much larger range of γ even when it might be difficult to measure in the outcrop. For instance, de Rosa et al. (1996) have shown that the basal parts of a lava flow can reach values of $\gamma \sim 80$, whereas the deformation in the central part of the same flow remains at $\gamma \lesssim 10$. Similar ranges of shear deformation can be expected in dikes or other tabular intrusions.

Such a difference in the range of interest in the values of γ, in combination with the results of our model calculations, allow us to define threshold values controlling the expected fabric in different geologic settings. For example, by using the results shown in Fig. 8, we can establish that markers with an elongation ratio <0.25 will have attained a stable orientation in most cases where deformation of a solid rock is considered. Particles with an elongation ratio between 0.25 and 0.55 may have reached this stage if deformation is ~ 5, whereas even more spherical particles may be considered to have reached a stable orientation if the amount of deformation undergone by the rock is small ($\gamma < 4$). Similar threshold values for the elongation ratio have been proposed by Piazolo et al. (2002) and Pennacchioni et al. (2001) based on experimental and empirical observations, respectively.

Also, it is noted that due to the different rotation periods

of the particles as a function of their elongation ratio, the model predicts that two mineral species, each with a characteristic shape, should achieve different degrees of alignment for the same amount of rock-deformation, therefore resulting in the formation of different mineral subfabrics in the rock. As suggested by Fernandez and Fernández-Catuxo (1997) the adequate identification of such subfabrics in a rock can be used to constrain the total amount of shear experienced by the rock in the absence of other indicators.

Situations in which fabric acquisition involves a deforming rock that is liquid in the everyday sense of the term (i.e. magma or lava during flow), however, present a more complex scenario in which commonly it is almost impossible to estimate the value of γ that is represented by a given mineral fabric. We examine these cases with more detail in the next section.

5.2. Mineral fabrics and flow direction of magma in dikes and in lava flows

Our results indicate that although some cyclicity will be present for any elongation ratio (considering that γ might be too large), it is much more probable to find an average orientation of grains parallel to flow direction if the grains have an elongation ratio <0.25 than it is to find them along any other direction. For this reason it is concluded that particles this elongated are reliable indicators of the direction of shear in almost any geological situation. As the value of r increases, however, the evolution of the system has two features that must be evaluated carefully before making an interpretation in terms of flow direction. On the one hand, the cyclic movement of the system becomes more and more important, so that an imbrication contrary to the flow direction can be achieved during some stages of deformation. On the other hand, our calculations show that it becomes probable to find mineral fabrics in which the average orientation of the grains forms an angle with the flow direction depending on the initial distribution of axes. In some extreme cases, the angle between the cluster of particle axes and flow direction can be nearly 90°. These features undoubtedly introduce some noise in the interpretation of mineral fabric as an indicator of flow direction, but based on our results it is possible to assess the relationship that exists among the mean direction of the particles, the flow direction, the plane of flow and the orientation of the velocity gradient by examining a series of different particle systems (as for example rock samples collected a few centimeters from each other) within the same rock.

Further, it is noted that although possible, such deviations from the 'normal' case (i.e. axes parallel to flow direction or imbricated in the right angle) are not very common. From 600 runs studied in detail encompassing elongation ratios between 0.05 and 0.95, Chávez-Álvarez (2003) only documented 129 ($\sim$20%), which resulted in a mean direction of the whole cycle that is significantly different from the true flow direction. Additionally, by noticing that the more anisotropic distributions commonly correspond to the cases where the mean is closer to flow direction, the probability of finding a significant flow direction from these data might be increased by eliminating the samples with weaker fabric strengths before calculating a mean from all the samples. Finally, it is noted that systematic variation of mean orientations obtained from parts of the flow likely to have experienced slightly different shear rates (as for example at different distances from a dyke wall) can help to identify the occurrence of a sample that is the result of a particle system with an anomalous orientation of the mean.

5.3. Influence of the 3D shape of particles and of mechanical interactions during deformation

The effect of departure of the particles from an axial shape in their motion during flow has been documented by some authors (Hinch and Leal, 1979; Freeman, 1985; Iezzi and Ventura, 2002). The three-dimensionality of the particle shapes results in the loss of cyclic behavior, and may lead to a chaotic movement. However, as shown by Iezzi and Ventura (2002), prism- and tablet-shaped minerals achieve a stable fabric orientation upon shearing, whereas cubic minerals oscillate periodically. These results are equivalent to those obtained in our models if we compare prisms and tablets with particles of $r \sim 0.1$ and cubes with particles of $r \sim 1$. Thus, although our model is based on axisymmetric particles, it is concluded that the three-dimensionality of particle shape does not affect the basic behavior of a multiparticle system here described.

On the contrary, the mechanical interactions between neighboring particles upon deformation is likely to influence dramatically the behavior of the system. The main effect of mechanical interactions, as revealed by analogue experiments (Ildefonse et al., 1992, 1997; Arbaret et al., 1996, 1997; Fernandez and Fernández-Catuxo, 1997) is to increase the period of rotation of the particles, so that a stable orientation is eventually achieved; the larger the concentration of particles in the deforming rock the more marked the effects of interactions in the final fabric. Although concentrations as low as 13–14% are likely to influence fabric development in some cases (Arbaret et al., 1996), there are situations in which the concentration of particles during movement remained well below these values (e.g. Castro et al., 2002). Therefore, there are some natural situations in which mechanical interactions between particles can be neglected, and in which our model will be directly applicable.

6. Conclusions

Our modeling results have shown that both the elongation ratio of individual particles and the initial

distribution of their axes are important in controlling the acquisition of a stable fabric upon deformation. By having analyzed the whole range of particle elongations we were able to fill the gaps that existed between the results of Manga (1998) and Reed and Tryggvason (1974), showing that indeed the very elongated particles used by Manga (1998) were responsible for the acquisition of a stable fabric within the range of shear considered by him. Our study also shows that the more elongated particles ($r < 0.2$) will be, in general, reliable indicators of the sense of shear because a system composed of such particles acquires a stable orientation with very little amounts of deformation, and keeps such fabric as shear increases to moderate values. Particles with larger elongation ratios ($0.2 < r < 0.5$) can also be of some utility if deformation remains moderate ($4 < \gamma < 10$). More importantly, the results of our model show that even more equant particles ($r > 0.5$) can be considered to have acquired a stable orientation if deformation remains low ($\gamma < 3$). In consequence, the interpretation of SPO measurements must take into consideration the amount of deformation that is suspected to have affected a given rock, and the elongation ratio of the particles under examination.

In the case of magmatic deformation, our results show that for equant particles it is possible to find mineral fabrics that have the wrong imbrication angle (relative to magma flow direction) or whose imbrication angle is very large (up to 90°). These departures from the 'normal' case are entirely due to the evolution of the system during magma flow, and are not necessarily due to turbulence or post-emplacement alteration effects. However, the occurrence of these cases is small relative to the occurrence of a normal fabric. Consequently, the occurrence of such departures does not preclude the use of SPO to determine flow directions provided that attention is given to systematic variations of fabrics across a flowing unit.

Acknowledgements

We thank the comments made by M. Ort, D.A. Ferrill and an anonymous reviewer that helped to improve the quality of the presentation. The additional support provided by the Dirección General de Posgrado of CICESE to M.J. Chávez-Álvarez allowing her to take part on the final stages of this paper is also greatly appreciated.

References

Arbaret, L., Diot, H., Bouchez, J.L., 1996. Shape fabrics of particles in low concentration suspensions: 2D analogue experiments and application to tiling in magma. Journal of Structural Geology 18, 941–950.

Arbaret, L., Diot, H., Bouchez, J.L., Lespinasse, P., de Saint-Blanquat, M., 1997. Analogue 3D simple-shear experiments of magmatic biotite subfabrics. In: Bouchez, J.L., Hutton, D.H.W., Stephens, W.E. (Eds.), Granite: from Segregation of Melt to Emplacement Fabrics, Petrology and Structural Geology, 8. Kluwer Academic Publishers, Dordrecht, pp. 129–143.

Bretherton, F.P., 1962. The motion of rigid particles in shear flow at low Reynolds number. Journal of Fluid Mechanics 14, 284–304.

Cañón-Tapia, E., Chávez-Álvarez, M.J., 2004. Theoretical aspects of particle movement in flowing magma: implication for the anisotropy of magnetic susceptibility of dykes and lava flows. In: Martin Hernandez, F., Aubourg, C., Jackson, M., Luneburg, C. (Eds.), Magnetic Fabric Methods and Applications. Geological Society, London, in press.

Castro, J., Manga, M., Cashman, K.V., 2002. Dynamics of obsidian flows inferred from microstructures: insights from microlite preferred orientations. Earth and Planetary Science Letters 199, 211–226.

Chávez-Álvarez, M.J., 2003. Evaluación de modelos físicos de anisotropía de susceptibilidad magnética para determinar direcciones de flujo de magma en diques. Unpublished Master's thesis, CICESE.

Dragoni, M., Lanza, R., Tallarico, A., 1997. Magnetic anisotropy produced by magma flow: theoretical model and experimental data from Ferrar dolerite sills (Antartica). Geophysical Journal International 128, 230–240.

Fernandez, A., 1987. Preferred orientation developed by rigid markers in two-dimensional simple shear strain: a theoretical and experimental study. Tectonophysics 136, 151–158.

Fernandez, A., Fernández-Catuxo, J., 1997. 3D biotite shape fabric experiments under simple shear strain. In: Bouchez, J.L., Hutton, D.H.W., Stephens, W.E. (Eds.), Granite: from Segregation of Melt to Emplacement Fabrics, Petrology and Structural Geology, 8. Kluwer Academic Publishers, Dordrecht, pp. 145–157.

Fernandez, A., Feybesse, J.L., Mezure, J.F., 1983. Theoretical and experimental study of fabrics developed by different shaped markers in two-dimensional simple shear. Bulletin de la Societe Geologique de France 25, 319–326.

Freeman, B., 1985. The motion of rigid ellipsoidal particles in slow flows. Tectonophysics 113, 163–183.

Gay, N.C., 1966. Orientation of mineral lineation along the flow direction in rocks: a discussion. Tectonophysics 3, 559–564.

Gay, N.C., 1968. The motion of rigid particles embedded in a viscous fluid during pure shear deformation of the fluid. Tectonophysics 5, 81–88.

Hinch, E.J., Leal, L.G., 1979. Rotation of small non-axisymmetric particles in a simple shear flow. Journal of Fluid Mechanics 92, 591–608.

Iezzi, G., Ventura, G., 2002. Crystal fabric evolution in lava flows: results from numerical simulations. Earth and Planetary Science Letters 200, 33–46.

Ildefonse, B., Launeau, P., Bouchez, J.L., Fernandez, A., 1992. Effect of mechanical interactions on the development of shape preferred orientations: a two-dimensional experimental approach. Journal of Structural Geology 14, 73–83.

Ildefonse, B., Arbaret, L., Diot, H., 1997. Rigid particles in simple shear flow: is their preferred orientation periodic or steady-state? In: Bouchez, J.L., Hutton, D.H.W., Stephens, W.E. (Eds.), Granite: from Segregation of Melt to Emplacement Fabrics, Petrology and Structural Geology, 8. Kluwer Academic Publishers, Dordrecht, pp. 177–185.

Jeffery, G.B., 1922. The motion of ellipsoidal particles immersed in a viscous fluid. Proceedings of the Royal Society London 102, 161–179.

Jezek, J., 1994. Software for modelling the motion of rigid triaxial ellipsoidal particles in viscous flow. Computers and Geosciences 20, 409–424.

Jezek, J., Melka, R., Schulmann, K., Venera, Z., 1994. The behaviour of rigid triaxial ellipsoidal particles in viscous flows—modeling of fabric evolution in a multiparticle system. Tectonophysics 229, 165–180.

Manga, M., 1998. Orientation distribution of microlites in obsidian. Journal of Volcanology and Geothermal Research 86, 107–115.

Pennacchioni, G., Di Toro, G., Mancktelow, N.S., 2001. Strain-insensitive preferred orientation of porphyroclasts in Monte Mary myonite. Journal of Structural Geology 23, 1281–1298.

Pfiffner, O.A., Ramsay, J.G., 1982. Constraints on geological strain rates: arguments from finite strain states of naturally deformed rocks. Journal of Geophysical Research 87, 311–321.

Piazolo, S., Bons, P.D., Passchier, C.W., 2002. The influence of matrix rheology and vorticity on fabric development of populations of rigid objects during plane strain deformation. Tectonophysics 351, 315–329.

Reed, L.J., Tryggvason, E., 1974. Preferred orientations of rigid particles in a viscous matrix deformed by pure shear and simple shear. Tectonophysics 24, 85–98.

de Rosa, R., Mazzuoli, R., Ventura, G., 1996. Relationships between deformation and mixing process in lava flows: a case study from Salina (Aeolian Islands, Thyrrenian Sea). Bulletin of Volcanology 58, 286–297.

Smith, J.V., 2002. Structural analysis of flow-related textures in lavas. Earth Science Reviews 57, 279–297.

Woodcock, N.H., 1977. Specification of fabric shapes using an eigenvalue method. Bulletin of the Geological Society of America 88, 1231–1236.